

**ROYAL SOCIETY
OPEN SCIENCE**

**Temporal and phylogenetic evolution of the sauropod
dinosaur body plan**

Journal:	<i>Royal Society Open Science</i>
Manuscript ID	RSOS-150636.R1
Article Type:	Research
Date Submitted by the Author:	24-Feb-2016
Complete List of Authors:	Bates, Karl; University of Liverpool, Musculoskeletal Biology Group Mannion, Philip; Imperial College London Falkingham, Peter; Liverpool John Moores University, School of Natural Sciences and Psychology Brusatte, Stephen Hutchinson, John; Royal Veterinary College Otero, Alexandros; Museo de La Plata, Sellers, William; University of Manchester, Faculty of Life Science Sullivan, Corwin; Institute of Vertebrate Paleontology and Paleoanthropology Stevens, Kent; University of Oregon Allen, Vivian; Royal Veterinary College
Subject:	evolution < BIOLOGY, biomechanics < BIOLOGY, palaeontology < BIOLOGY
Keywords:	biomechanics, computer modelling, centre-of-mass, body shape, phylogeny, gigantism
Subject Category:	Biology (whole organism)

SCHOLARONE™
Manuscripts

1
2 1 **Temporal and phylogenetic evolution of the sauropod dinosaur body plan**

3
4 2

5
6 3 Karl T. Bates^{1*}, Philip D. Mannion², Peter L. Falkingham³, Stephen L. Brusatte⁴, John R.

7
8 4 Hutchinson⁵, Alejandro Otero⁶, William I. Sellers⁷, Corwin Sullivan⁸, Kent A. Stevens⁹ & Vivian

9
10 5 Allen⁵.

11
12 6

13
14 7 ¹Department of Musculoskeletal Biology, Institute of Aging and Chronic Disease, University of
15 8 Liverpool, The Apex Building, 6 West Derby Street, Liverpool L7 8TX, UK;

16
17 9 ²Department of Earth Science and Engineering, Imperial College London, South Kensington
18 10 Campus, London SW7 2AZ, UK;

19
20 11 ³School of Natural Sciences and Psychology, Liverpool John Moores University, James Parsons
21 12 Building, Bryon Street, Liverpool, L3 3AF, UK.

22
23 14 ⁴School of GeoSciences, University of Edinburgh, Grant Institute, The King's Buildings, James
24 15 Hutton Road, Edinburgh, EH9 3FE, UK;

25
26 16 ⁵Department of Comparative Biomedical Sciences, Structure & Motion Laboratory, Royal
27 17 Veterinary College, University of London, Hatfield, Hertfordshire, AL9 7TA, UK;

28
29 18 ⁶CONICET – División Paleontología de Vertebrados, Museo de La Plata, Paseo del Bosque s/n,
30 19 La Plata, B1900FWA, Argentina;

31
32 21 ⁷Faculty of Life Sciences, University of Manchester, Michael Smith Building, Oxford Road,
33 22 Manchester, M13 9PT, UK;

34
35 24 ⁸Key Laboratory of Vertebrate Evolution and Human Origins, Institute of Vertebrate
36 25 Paleontology and Paleoanthropology, Chinese Academy of Sciences, 142 Xizhimenwai Dajie,
37 26 Beijing 100044, China;

38
39 28 ⁹Department of Computer and Information Science, University of Oregon, Eugene, Oregon,
40 29 97403, USA;

41
42 32 *Correspondence to: k.t.bates@liverpool.ac.uk.

43
44 33 **Key words:** biomechanics, computer modelling, centre-of-mass, body shape, phylogeny,
45 34 gigantism.

1
2
3
4
5
6
7
8
9
10
11
12
13
14
15
16
17
18
19
20
21
22
23
24
25
26
27
28
29
30
31
32
33
34
35
36
37
38
39
40
41
42
43
44
45
46
47
48
49
50
51
52
53
54
55
56
57
58
59
60

35 SUMMARY

36 The colossal size and body plan of sauropod dinosaurs are unparalleled in terrestrial
37 vertebrates. However, to-date there have been only limited attempts to examine temporal and
38 phylogenetic patterns in the sauropod bauplan. Here we combine three-dimensional
39 computational models with phylogenetic reconstructions to quantify the evolution of whole-
40 body shape and body segment properties across the sauropod radiation. Limitations
41 associated with the absence of soft tissue preservation in fossils result in large error bars
42 about mean absolute body shape predictions. However, applying any consistent
43 skeleton:body volume ratio to all taxa does yield changes in body shape that appear
44 concurrent with major macroevolutionary events in sauropod history. A caudad shift in
45 centre-of-mass in Middle Triassic Saurischia, associated with the evolution of bipedalism in
46 various dinosaur lineages, was reversed in Late Triassic sauropodomorphs. A craniad centre-
47 of-mass shift coincided with the evolution of quadrupedalism in the Late Triassic, followed by
48 a more striking craniad shift in Late Jurassic–Cretaceous titanosauriforms, which included the
49 largest sauropods. These craniad CoM shifts are strongly correlated with neck enlargement, a
50 key innovation in sauropod evolution and pivotal to their gigantism. By creating a much larger
51 feeding envelope, neck elongation is thought to have increased feeding efficiency and opened
52 up trophic niches that were inaccessible to other herbivores. However, we find that relative
53 neck size and centre-of-mass position are not strongly correlated with inferred feeding habits.
54 Instead the craniad centre-of-mass positions of titanosauriforms appear closely linked with
55 locomotion and environmental distributions, potentially contributing to the continued
56 success of this group until the end-Cretaceous, with all other sauropods having gone extinct
57 by the early Late Cretaceous.

1
2 59 **INTRODUCTION**
3
4

5 60 Sauropod dinosaurs were the dominant group of large herbivores in global terrestrial
6
7 61 ecosystems throughout much of the Mesozoic [1-2]. Their gigantic body sizes, an order of
8
9 62 magnitude greater than any living terrestrial animal, in combination with a body plan distinct
10
11 63 among tetrapods (e.g. long muscular necks and tails; graviportal, columnar limbs) make them
12
13 64 a unique group for studies of morphological and functional evolution through deep time [3].
14
15 65 In particular, the evolution of sauropods from relatively small-bodied bipedal, and possibly
16
17 66 facultatively bipedal, ancestors into extremely large-bodied obligate quadrupeds involved
18
19 67 fundamental changes to most aspects of their biology [3]. However, despite numerous studies
20
21 68 linking changes in biodiversity, ecology and biomechanics to body size and shape (e.g. [3-6]),
22
23 69 there is a clear lack of quantitative analysis of temporal and phylogenetic trends in the
24
25 70 sauropod bauplan.
26
27
28
29
30

31 71 Simple bone and body length segment ratios have been used to quantify aspects of
32
33 72 body shape diversity across Sauropoda [7]. Studies that have sought to more directly quantify
34
35 73 three-dimensional body shape in sauropods [5-6] have been hampered by small sample sizes.
36
37 74 In particular very few Titanosauriformes, which dominated sauropod faunas throughout the
38
39 75 Cretaceous [2], with derived members being the only sauropods to survive up to the end-
40
41 76 Cretaceous mass extinction [1-2], have been subject to body shape analysis due to the absence
42
43 77 of well-preserved specimens. The group includes famous taxa such as *Brachiosaurus*, as well
44
45 78 as the largest known sauropods, such as the gigantic *Argentinosaurus* [1-3]. Therefore, we
46
47 79 currently have very little understanding of how the unprecedented body plans of
48
49 80 titanosauriforms contributed to their success in the latter half of the 150 million year
50
51 81 evolutionary history of sauropods (Fig 1).
52
53
54
55
56
57
58
59
60

1
2 83 In this study we attempt to rectify this by estimating parameters for overall body
3
4 84 morphology (mass, centre-of-mass [CoM] and first mass moments [FMM, mass multiplied by
5
6 85 CoM position]), both at whole-body and body segment levels for exemplar taxa covering the
7
8 86 temporal and phylogenetic extent of the sauropod radiation (sauropods, basal
9
10 87 sauropodomorphs and their immediate antecedents spanning the Middle Triassic through to
11
12 88 the end-Cretaceous; Fig 1) using automated computational volumetric techniques [9-10] (Fig
13
14 89 2). Specimens of 17 sauropodomorph taxa and an additional five extinct and extant outgroup
15
16 90 taxa were chosen (Fig 1). Crucially our analysis includes a number of Cretaceous
17
18 91 titanosauriforms, made possible by recent discoveries of near-complete specimens and
19
20 92 through careful sensitivity analysis of less complete taxa. Indeed, herein we conduct an
21
22 93 exhaustive sensitivity analysis of numerous parameters associated with volumetric
23
24 94 reconstruction (building on our previous work [9-14]), allowing us to quantitatively
25
26 95 demonstrate keys areas of uncertainty in our models and subsequently to qualitatively gauge
27
28 96 confidence in our ability to reconstruct macroevolutionary patterns within sauropodomorph
29
30 97 dinosaurs.

31
32
33
34
35
36
37 98 To address temporal and phylogenetic patterns directly, rather than just using values
38
39 99 for the studied sauropods, we mapped normalized estimated parameters from our volumetric
40
41 100 models onto the evolutionary splitting events or nodes shown in Figure 1 (based on [15]),
42
43 101 using temporal branch lengths and a Brownian maximum-likelihood evolutionary model. This
44
45 102 approach furthermore allows us to identify associations between morphological patterns in
46
47 103 whole-body CoM and segment-specific parameters, and place changes in these fundamental
48
49 104 biological properties in the context of existing hypotheses regarding functional, ecological and
50
51 105 macroevolutionary patterns within sauropodomorphs.
52
53
54
55

56 106
57
58
59
60

1
2 107 **Material and Methods**
3
4

5 108 **Taxonomic coverage:** Our sample of taxa (Fig. 1) covers the full temporal extent of the
6
7 109 sauropod radiation (sauropods, basal sauropodomorphs and their immediate antecedents,
8
9 110 spanning the Middle Triassic through to the end-Cretaceous). Phylogenetically, all major sub-
11
12 111 clades are represented, with the exception of Rebbachisauridae. Very few sauropodomorphs
13
14 112 are represented by individuals with highly complete skeletons. Indeed volumetric
15
16 113 reconstructions of dinosaurs in general rely heavily on composite skeletons produced by
17
18 114 scaling elements from multiple individuals and estimating the dimensions of unpreserved
19
20 115 elements using crude geometric proxies or reconstructions in cast/sculpted material. In the
21
22 116 Electronic Supplementary Material (ESM1) we review skeletal completeness in our sample of
23
24 117 sauropodomorph taxa before exploring its impact on our results in a number of different
25
26 118 ways through several sensitivity analyses (see below).
27
28
29
30
31 119

32
33
34 120 **Volumetric Reconstruction Approach:** Three-dimensional models of complete to near-
35
36 121 complete skeletons of taxa (Fig 1; see also ESM1) were digitized using either long-range laser
37
38 122 scanning [9-12], digital photogrammetry [16], or CT scanning in the case of *Alligator*. The
39
40 123 model of *Camarasaurus* was generated through computer-aided design approaches described
41
42 124 in Stevens [17]. To quantify body proportions and overall body shape, CoM position and body
43
44 125 segment masses were estimated from computer reconstructions of gross morphology built
45
46 126 around digitized skeletons using a convex hulling approach [9-10]. Each 3D skeletal model
47
48 127 was posed in a standard reference posture, with the tail and neck extending horizontally and
49
50 128 the limbs in a fully extended, vertical position (Fig 2, Movie S1). Models were then divided
51
52 129 into standardized body segments and the minimum convex hull (enclosed volume) around
53
54 130 each segment calculated using the MATLAB (www.mathworks.com) qhull algorithm [9-10].
55
56
57
58
59
60

1
2 131 This mathematical approach of tight fitting 3D convex polygons to each body segment
3
4 132 minimizes subjectivity in body volume reconstruction. Also, the extent of an object's convex
5
6 133 hull is dictated solely by its geometric extremes, which minimizes impact of reconstructed (i.e.
7
8 134 missing) skeletal components in the mounted skeletons (see the ESM in [10] for extensive
9
10 135 discussion of this, and further discussion below and in ESM1 here).

11
12
13 136

14
15 137 The minimum convex hull volumes provide the minimum volume estimate for each animal,
16
17 138 and a baseline for our sensitivity analyses in which we generated further models (Fig 2; see
18
19 139 also MovieS1). In our first model iteration, the minimal convex hulls were geometrically
20
21 140 expanded by 21%, following a previous study on extant mammalian body proportions [9]. We
22
23 141 subsequently generated a 'maximal mass model' in which the volume of the trunk segment
24
25 142 was increased by 50%, and the volumes of all other segments by 100% [10]. From these three
26
27 143 models we produced two further models composed of the combination of segments that
28
29 144 produced the most cranial and most caudal CoM positions (Fig 2, Movie S1). The 'maximal'
30
31 145 volumetric expansions yielded an overall increase in body volume of around 60% in most of
32
33 146 the sauropods modelled, which is well in excess of the upper 95% confidence intervals
34
35 147 (corresponding to a 32.2% expansion) found for mammals by Sellers et al. [9]. Indeed, our
36
37 148 100% expansion of head, neck, tail and all limb segments are more than three times greater
38
39 149 than the upper 95% confidence interval from Sellers et al. [9]. Our maximum caudal and
40
41 150 cranial models are therefore composed of volumes that contain extremely large volumes at
42
43 151 one end of the animal and minimum convex hulls that can unequivocally be considered to
44
45 152 underestimate body segment volumes at the opposite end (Fig 2, Movie S1). Our decision to
46
47 153 generate such large error bars through these extreme models reflects our cautious approach
48
49 154 to volumetric reconstructions (e.g. [9-14]), the additional uncertainty associated with
50
51 155 reconstructed dinosaur body volumes (e.g. different body shapes and sizes to living animals),
52
53 156 and the goal to incorporate additional error margins to account for the more modest effects of
54
55
56
57
58
59
60

1
2 157 skeletal articulation and incompleteness (e.g. [10, 12]). To place the magnitude of these error
3
4 158 bars into relative context we also calculated the CoM of two model iterations using the upper
5
6 159 and lower 95% confidence intervals convex hull expansion from [9]. Specifically, a caudal CoM
7
8 160 model was derived by expanding caudal body segments (e.g. tail, hindlimbs) by the upper
9
10 161 95% confidence interval expansion (32.2%) and cranial body segments (e.g. forelimbs, neck,
11
12 162 head) by the lower 95% confidence interval expansion (9.01%). Reversing these expansions
13
14 163 yielded a cranial CoM model.
15
16

17
18 164

19
20 165 To further quantify likely error and evaluate the robustness of our conclusions regarding CoM
21
22 166 and body segment evolution, we also carried out additional sensitivity tests. These sensitivity
23
24 167 tests focus on the size of reconstructed zero-density respiratory volumes and errors
25
26 168 associated with skeletal completeness in specific taxa, which is particularly key to our analysis
27
28 169 of Cretaceous titanosauriforms. For example, neck length in *Dreadnoughtus* is poorly
29
30 170 constrained by fossilized remains, whereas in *Sauroposeidon* and *Neuquensaurus* composite
31
32 171 neck reconstructions have been produced from different specimens. We therefore ran
33
34 172 additional analyses with the neck length of *Dreadnoughtus* altered by +/-20% and those of
35
36 173 *Sauroposeidon* and *Neuquensaurus* altered by +/-10% to reflect this uncertainty. A similar
37
38 174 approach was used to assess the sensitivity of CoM predictions to the size of zero-density
39
40 175 respiratory structures, neck shape and tail length (see Figs S6-12 in ESM1). Also, given the
41
42 176 disparity in neck orientation reconstructions for sauropods in the literature and ongoing
43
44 177 controversy regarding this important issue [17-21], we carried out a sensitivity analysis on
45
46 178 neck posture (Fig 3). Some derived sauropods (macronarians) have been suggested by some
47
48 179 workers to have had more raised or inclined neck postures (e.g. [19-20]) We therefore ran
49
50 180 two sensitivity analyses related to neck orientation; one in which the neck segments of all
51
52 181 macronarians were rotated dorsally by 45 degrees (Fig 3a), and a second one in which the
53
54 182 neck of *Giraffatitan* was posed in the osteologically straight, undeflected state (Fig 3b) [17].
55
56
57
58
59
60

1
2 183 Note that in the simple “necks inclined to 45 degrees” models all other body segments
3
4 184 remained posed in the standardised postures used throughout this analysis. Applying this
5
6 185 rotation to the models in the postures in actual mounted skeletons results in a much higher
7
8 186 neck angle relative to the ground (e.g. around 68 degrees to the horizontal in *Giraffatitan*).
9
10 187 Exclusion of any curvature (e.g. S-shaped ‘swan-like’ curvature) also maximized the neck and
11
12 188 head CoM displacements in these models. Thus are we confident that our models cover the
13
14 189 range of habitual neck postures postulated for sauropods to-date [17-21].
15
16
17
18 190
19
20 191 In all model iterations the masses of all segments were calculated using a density of 1000 kg
21
22 192 m³. However, zero-density respiratory structures in the head, neck and ‘trunk’ segments were
23
24 193 reconstructed using surfaces lofted through NURBS circles that we shaped around the skeletal
25
26 194 models (e.g. around the centra and ribs in the trunk segment), and we subtracted the volume
27
28 195 of these structures from their overall segment volume before mass calculation, as in previous
29
30 196 studies [10-14]. To account for the impact of skeletal pneumaticity on mass properties, we
31
32 197 used convex hulling to enclose the volume of the centra of the cervical and dorsal vertebrae in
33
34 198 each of the modelled sauropodomorph taxa, although this approach undoubtedly
35
36 199 overestimates actual skeletal volume in these regions due to inter-articular spaces between
37
38 200 bones. We then recalculated the mass of the neck and thoracic segments accordingly, giving
39
40 201 the respiratory volume a density of 0 kg m³ and the pneumatic bone volume a density of 900
41
42 202 kg m³ (e.g. equating to an air space volume [22] of 50% if the density of air is 0 kg m³ and the
43
44 203 density of bone is assumed to be 1800 kg m³). To our knowledge, no study has explicitly
45
46 204 quantified the impact of pneumaticity on the 3D mass properties of a living archosaur, nor is
47
48 205 there sufficient information in the literature at present to attribute differential levels of
49
50 206 pneumatic air space volume within or between whole-body reconstructions of individual
51
52 207 sauropod taxa. We therefore chose this simplified, standardized approach within our
53
54 208 sauropodomorph models for our phylogenetic statistical analysis (see below). However, to
55
56
57
58
59
60

1
2 209 provide the first insight into the potential nature and magnitude of differential pneumaticity
3
4 210 on 3D mass properties we also report the raw results from an additional sensitivity analysis
5
6 211 in which we varied the density value attributed to the convex hull bone volumes in the
7
8 212 thoracic and neck segments.
9

10 213

11
12
13 214 ***Phylogenetic and statistical analysis:*** We normalized estimated CoM positions and segment
14
15 215 properties (segment lengths, masses and CoM positions) by division by either mean estimated
16
17 216 whole-body mass (for masses) or by mean estimated whole-body mass^{1/3} (for linear
18
19 217 parameters). We then used a simplified, high-level phylogeny of the sauropod branch of
20
21 218 Archosauria (Fig 1), with branch lengths based on first-occurrence data for fossils of each
22
23 219 group, as the basis for estimation of ancestral node-states for each parameter over the course
24
25 220 of sauropod evolution (see ESM1). As this approach often leads to branch lengths of zero,
26
27 221 between first-occurrence taxa from the same geological formation, or due to ghost-range
28
29 222 issues, we substituted all zero branch lengths with lengths of one million years. Sensitivity
30
31 223 tests surrounding this assumption (see Figs 2-3 in ESM1) did not qualitatively affect our
32
33 224 conclusions.
34
35
36
37
38
39

40 225

41 226 The phylogeny and normalized data were then used as input to estimate ancestral node states
42
43 227 with the ape package [23] for R (version 3.02 [2013-09-25], [http://cran.r-](http://cran.r-project.org/web/packages/ape/)
44
45 228 [project.org/web/packages/ape/](http://cran.r-project.org/web/packages/ape/)). Due to better performance with variable (and long) branch
46
47 229 lengths, the established method of ACE estimation using maximum likelihood and a simple
48
49 230 Brownian evolutionary model were chosen over the older method of maximum parsimony, or
50
51 231 the less-established method of generalized least squares. To test for phylogenetic signal in
52
53 232 our parameters, we used the same simplified phylogeny and normalized data to generate
54
55 233 Pagel's Lambda scores (λ) with the phytools package [24] for R ([http://cran.r-](http://cran.r-project.org/web/packages/phytools/)
56
57 234 [project.org/web/packages/phytools/](http://cran.r-project.org/web/packages/phytools/)). To assess the degree of correlation between our
58
59
60

1
2 235 parameters, we first calculated phylogenetic independent contrasts (PIC's, [25]) from our raw
3
4 236 (un-normalized) data and phylogeny, again using the ape package for R. PIC's for parameters
5
6 237 were then tested for correlation using Spearman's Rho test (ρ , a nonparametric test was used
7
8 238 due to non-normality in several parameters), performed using the Hmisc package for R
9
10 239 (<http://cran.r-project.org/web/packages/Hmisc/index.html>). All signals and correlations
11
12 240 were accepted as significant using an alpha level of 0.05. All raw and normalized mass
13
14 241 property data are tabulated in ESM1 and our convex hull volumes and ACE outputs are freely
15
16 242 available from <http://datadryad.org/review?doi=doi:10.5061/dryad.1qp47>.
17
18
19
20
21 243
22
23

24 244 **Results**

25
26
27 245 Figure 4 shows the raw CoM predictions from the three model iterations (initial, max cranial
28
29 246 and max caudal) for all taxa with normalization conducting using distance cranial to the hip
30
31 247 divided by body mass^{0.33} (Fig 4a) and as a fraction of gleno-acetabular distance (Fig 4b). Raw
32
33 248 CoM predictions with different degrees of skeletal pneumaticity in the neck and thoracic body
34
35 249 segments are also shown (Fig 4). Figure 5 shows reduced major axis (RMA) regression of raw
36
37 250 CoM data against body mass for three taxonomic groups (all taxa, sauropodomorphs only, and
38
39 251 sauropods only), again normalized by (Fig 5a) distance cranial to the hip divided by body
40
41 252 mass^{0.33} and (Fig 5b) as a fraction of gleno-acetabular distance. In both cases we find a weak
42
43 253 positive linear relationship between relative CoM positions and body mass (Fig 5).
44
45
46
47
48
49 254
50
51

52 255 Analysis of our ancestral state estimations (ACE) mean CoM data using Pagel's Lambda (λ)
53
54 256 suggests a significant phylogenetic signal ($\lambda = 0.86$) in CoM over sauropod evolution (Fig 6).
55
56 257 Qualitative assessment of our ACE for mean CoM over sauropod evolution suggests three
57
58
59
60

1
2 258 trends (Fig 6). Firstly, in the Middle Triassic (~245 Ma to ~230 Ma) we find a caudad CoM
3
4 259 shift from the ancestral position (~0.3 gleno-acetabular lengths from the hip) in basal
5
6 260 dinosauromorphs to a minimum of ~0.2 gleno-acetabular lengths from the hip in Saurischia
7
8 261 (Fig 6). This shift coincides with, and is plausibly associated with, the onset and progressive
9
10 262 evolution of bipedalism in various dinosaur lineages. Secondly, we find a subsequent, steady
11
12 263 craniad shift in the Late Triassic and Early–Middle Jurassic (~230 Ma onwards), reaching
13
14 264 ~0.45 gleno-acetabular lengths from the hip in Middle Jurassic sauropods (Fig 6). This shift
15
16 265 coincides with, and is plausibly associated with, the evolution of obligate quadrupedalism [15]
17
18 266 and increased body size in the early sauropods. Thirdly, we find a noticeable craniad shift in
19
20 267 the Late Jurassic (~161 Ma) reaching (~0.55 gleno-acetabular lengths from the hip in early
21
22 268 Titanosauriformes (Fig 6), represented by the brachiosaurid *Giraffatitan* (Fig 1). This craniad
23
24 269 mean CoM position is maintained within the brachiosaurid sister clade Somphospondyli
25
26 270 (including the titanosaurian radiation), and thus in all titanosauriform lineages that survived
27
28 271 into the Cretaceous (Figs 1, 6).
29
30
31
32
33
34
35
36
37

272

38 273 Analysis of correlation in PICs using Spearman's Rho (ρ) indicates that the strongest
39
40 274 significant correlations were found between mean whole-body CoM position (Fig 6) and the
41
42 275 first mass moment (FMM, the product of segment mass and segment CoM) of the neck
43
44 276 segment (ρ 0.98, Fig 7d). Analysis of significant correlation in the components of neck FMM
45
46 277 (Fig 7b-c), suggests that changes in both neck CoM position (ρ 0.97) and neck mass (ρ 0.94)
47
48 278 were similarly important to the effects of the neck on whole-body CoM position. Still
49
50 279 significant but less strongly correlated was neck length (ρ 0.80), although this parameter
51
52 280 cannot be fully separated from CoM position, barring considerable morphological change.
53
54 281 Head CoM position (obviously strongly related to neck morphology) also shows a positive
55
56 282 association with whole-body CoM (ρ 0.93; Fig 7c).
57
58
59
60

1
2 283

3
4
5 284 The next strongest association with a cranially shifted whole-body CoM that was found was an
6
7 285 increasing FMM of the thoracic segment (ρ 0.86; Fig 7*d*). Analysis of FMM components
8
9 286 suggests that changes in both segment mass (ρ 0.80; Fig 7*b*) and segment CoM position (ρ
10
11 287 0.78; Fig 7*c*), were similarly important to the effects of the thoracic segment on whole-body
12
13 288 CoM position. Interestingly, only a weak to moderate negative association is evident between
14
15 289 whole-body CoM and tail segment FMM (ρ -0.46, Fig 7*d*). Of the FMM components, only the
16
17 290 tail segment CoM shows a significant relationship (ρ -0.44, Fig 7*d*).
18
19

20
21
22 291

23
24
25 292 Significant correlation was also found between whole-body CoM and our two measures of
26
27 293 body size - estimated whole-body mass (ρ 0.83), and gleno-acetabular distance (ρ 0.65),
28
29 294 indicating that larger sauropods tend to have a more cranial whole-body CoM position, in
30
31 295 agreement with the relative weak trend seen in raw CoM data (Fig 5). Weaker, but still
32
33 296 notable, correlations were found between whole-body CoM and pectoral limb segment FMM
34
35 297 (ρ 0.69; Fig 7*d*), segment CoM position (ρ 0.77; Fig 7*c*), and segment mass (ρ 0.77; Fig 7*b*).
36
37 298 Pectoral limb length showed a similar correlation (ρ 0.68; Fig 7*a-b*). In the pelvic limb,
38
39 299 significant correlations were weaker, and recovered only for mass (ρ 0.60; Fig 7*b*) and length
40
41 300 (ρ 0.0.49; Fig 7). Additional discussion of patterns in individual body segment properties (Fig
42
43 301 7) can be found in the ESM.
44
45
46
47

48
49 302

50
51
52 303 Extensive additional sensitivity analyses (see ESM1, Figs S5-12) indicated that only neck
53
54 304 orientation and high degrees of skeletal incompleteness in the neck (i.e. uncertain total neck
55
56 305 length) have a noticeable impact on CoM evolution results (Fig 8; see also Figs S6-14). Re-
57
58 306 orienting all macronarian necks to highly inclined postures resulted in caudad and dorsad
59
60

1
2 307 shifts in whole-body CoM (Fig S5) and moderately weakened the notable cranial shift in CoM
3
4 308 seen in Late Jurassic titanosauriforms (Fig 8). Changing neck length in *Sauroposeidon*,
5
6 309 *Dreadnoughtus* and *Neuquensaurus* had a much smaller impact on CoM evolution (Fig 8), with
7
8 310 10-20% shorter necks in these taxa only slightly weakened the sharp cranial shift in Late
9
10 311 Jurassic titanosauriforms. Increasing neck length in these taxa exacerbated the
11
12 312 aforementioned pattern (Fig 8).

13
14
15
16 313

17 18 19 314 **Discussion**

20 21 22 315 ***(a) Sensitivity analyses and uncertainties in CoM estimations***

23
24
25 316 This analysis has a number of limitations that are largely inherent to studies of form and
26
27 317 function in fossil vertebrates. Convex hulling generates volumetric reconstructions that are
28
29 318 objectively based on the 3D size and shape of fossilized skeletons. Thus the patterns identified
30
31 319 in our initial 'mean' model iteration (Figs 4-6) are driven directly by similarities and
32
33 320 differences in the 3D size and shape of fossilized skeletons. However, the absence of soft
34
35 321 tissue preservation means we must accept high levels of uncertainty in quantitative estimates
36
37 322 of body size and shape (Figs 2, 4, 6). Indeed this is confounded further in many instances by
38
39 323 incomplete skeletal preservation, and herein we have both employed a method that
40
41 324 minimizes this effect as far as possible ([10]; see also ESM1) and additionally allows us to
42
43 325 acknowledge and quantify associated errors through careful sensitivity tests (Fig 8, Figs S5-
44
45 326 12), which is difficult if not impossible using more indirect, qualitative or subjective
46
47 327 approaches (e.g. [7]).

48
49
50
51
52 328

53
54 329 Our maximum caudal and cranial model iterations represent highly implausible, if not
55
56 330 untenable, body shape reconstructions, and the model iterations constructed using the 95%
57
58 331 confidence intervals associated with average mammalian convex hull expansion [9] likely
59
60

1
2 332 represent a more plausible approximation of volumetric error in our data (Fig 4, 6). If model
3
4 333 iterations constructed using the 95% confidence intervals associated with average
5
6 334 mammalian convex hull expansion [9] are accepted as maximal error models then the three
7
8 335 patterns in sauropodomorph CoM evolution noted above appear reasonably robust,
9
10 336 particularly when normalized by gleno-acetabular distance (Fig. 6b). However, these current
11
12 337 confidence intervals are based solely on mammalian taxa and clearly considerable data from
13
14 338 living non-mammalian taxa are required to establish a more exhaustive and robust confidence
15
16 339 intervals.
17
18
19
20 340

21
22 341 Our analysis provides the first quantitative insight into the potential nature and magnitude of
23
24 342 differential levels of skeletal pneumaticity on CoM positions in archosaurs (Fig 4). Wedel [22]
25
26 343 attempted to provide some quantitative estimates of the potential magnitude of overall mass
27
28 344 reduction in sauropods resulting from 'empty' air space in pneumatic vertebrae. Based on
29
30 345 measurements from individual vertebrae from a variety of sauropod taxa, Wedel [22]
31
32 346 suggested that air-space proportion (ASP, the proportion of internal bone volume occupied by
33
34 347 air) may have ranged between 0.32-0.89, and suggested "it seems reasonable to conclude that
35
36 348 most sauropod vertebrae contained at least 50% air, by volume." As yet there has been no
37
38 349 systematic study of how air-space proportion varies within the body of an individual
39
40 350 sauropod, or indeed across taxa that would inform (quantitatively) on temporal and
41
42 351 phylogenetic trends in ASP. We therefore mimicked the effect of differential ASP across our
43
44 352 sauropod taxa by varying the density of our approximated cervical and thoracic vertebrae
45
46 353 volumes across a range equivalent to 0.5-0.9 ASP (Fig 4). This analysis demonstrates that
47
48 354 increasing ASP in cervical and thoracic vertebrae yields more caudal CoM positions (as
49
50 355 expected), and indeed that highly differential degrees of ASP across taxa could potentially
51
52 356 alter relative CoM positions, thereby exacerbating or negating trends in CoM evolution seen
53
54 357 here (Figs 4, 6).
55
56
57
58
59
60

1
2 358
3
4 359 Alternative reconstructions of sauropods with poorly preserved necks did not, by themselves,
5
6 360 significantly impact ACE mean CoM predictions (Fig 8). However, neck posture in
7
8 361 macronarians (which does not exert an influence on our analysis of body proportions; Fig 7),
9
10 362 did have a much larger quantitative impact on CoM evolution, moderately weakening the
11
12 363 notable craniad shift in Late Jurassic titanosauriforms (Fig 8). However, again our alternate
13
14 364 neck postures were deliberately inclined by extreme amounts, beyond existing quantitative
15
16 365 estimates of habitual posture for individual taxa [17-18] and thus the data shown in Figure 8
17
18 366 represent an extreme representation of the neck posture effects (Fig 3) on CoM evolution.
19
20 367
21
22 368 Our sample of modeled taxa also represents only a small proportion of the total number of
23
24 369 sauropodomorph species currently described. However, our sample does include at least one
25
26 370 representative from each major sauropodomorph sub-clade, with the exception of
27
28 371 Rebbachisauridae (as noted above). Rebbachisauridae is currently known only from the mid-
29
30 372 Cretaceous and represents a basal clade of Diplodocoidea [1]. From within Rebbachisauridae,
31
32 373 only *Nigersaurus* is potentially complete enough for volumetric reconstruction and body
33
34 374 shape evaluation. Qualitative assessment of the skeleton of *Nigersaurus* suggests it would not
35
36 375 have impacted significantly on our results. *Nigersaurus* has 13 cervical vertebrae that are not
37
38 376 especially elongate [26] and so its neck is crudely similar to the short necks of dicraeosaurids
39
40 377 (one fewer cervical) and *Jobaria* (the same number of cervical vertebrae and immediate
41
42 378 outgroup to Neosauropoda in our study). Other titanosaurian sub-clades, not represented
43
44 379 herein, have been named in the literature, but none of these preserve suitably complete
45
46 380 skeletons, and most of these clades currently have limited support and comprise only a few
47
48 381 putative taxa [e.g. 27]. The 95% confidence intervals for our ACE mean CoM data provide a
49
50 382 measure of the uncertainty surrounding CoM predictions resulting from the inter-related
51
52 383 effects of taxon sampling and branch lengths (Fig 6). These suggest a notably higher degree of
53
54
55
56
57
58
59
60

1
2 384 uncertainty surrounding ACE CoM estimations for Titanosauria and Lithostrotia, reflecting
3
4 385 their relatively long branches lengths (Fig 1, Table S2; see Figs S2-3 for additional analysis).

5
6 386

7
8 387 As recognition of the high levels of uncertainty in our data (Figs 2, 4, 6, 8), resulting from
9
10 388 factors inherent to studies of evolutionary form-function in fossil vertebrates, we restrict
11
12 389 possible interpretations to large-scale trends in our data, which are supported by major
13
14 390 changes in the 3D proportions of fossilized skeletons (Fig 7) noting the limitations we have
15
16 391 highlighted where appropriate. We have made our volumetric reconstructions freely available
17
18 392 so that other workers can build on our analysis as new data become available, or so that
19
20 393 alternative methods for reconstructing or modifying segments and body shapes as well as
21
22 394 estimating phylogenetic patterns can be attempted.
23
24
25
26
27
28
29

30 395

31 396 ***(b) Temporal and phylogenetic patterns based on mean mass property data***

32
33 397 Our mean CoM data, and indeed any single model iteration shown in Figures 4-8 represent
34
35 398 volumetric reconstructions in which the skeletal:body volume ratio is standardised across
36
37 399 taxa. Thus in these cases patterns evident are driven directly by similarities and differences in
38
39 400 the 3D size and shape of fossilized skeletons. A highly elongate neck has been cited as “the
40
41 401 most important key innovation” in sauropod evolution [3]. Our new results reveal not only
42
43 402 the evolutionary variation of relative neck size in sauropods, but also the central, but
44
45 403 previously unquantified, role it played in the evolution of overall body shape and mass
46
47 404 distribution, which we quantitatively represent for the first time using inertial properties
48
49 405 (Figs 6-7). Traditionally, neck elongation has been considered critically important because it
50
51 406 potentially allowed more efficient food uptake by enabling a much larger feeding envelope,
52
53 407 making food accessible that was out of the reach of other herbivores [3, 17-21, 28]. Given the
54
55 408 apparent importance for feeding ecology, it is surprising (even given the relatively low sample
56
57
58
59
60

1
2 409 size herein) that neither relative neck sizes (Fig 7) nor whole-body CoM positions (Fig 6)
3
4 410 show any systematic correlation to skull functional morphology and inferred mechanics [29-
5
6 411 33]. Recent morphometric and biomechanical analysis have supported the existence of two
7
8 412 cranial morpho-functional types within Sauropoda: a 'broad-crowned' dental morphotype
9
10 413 with robust skulls adapted to acquiring and processing relatively coarser fodder, and a
11
12 414 'narrow-crowned' dental morphology with reduced dentition and jaw adductor musculature
13
14 415 that likely limited food choice [29]. At least some taxa displaying this latter morphotype have
15
16 416 been hypothesized to rely heavily on branch stripping through specialized neck motions [29-
17
18 417 30]. Our analyses show that both functional groups contain taxa with relatively long and short
19
20 418 necks: the 'narrow-crowned' group includes titanosaurs and diplodocids with relatively long
21
22 419 necks and other diplodocoids with relatively short necks, whereas the 'broad crowned' group
23
24 420 contains the extremely long-necked *Mamenchisaurus* and the shorter-necked *Camarasaurus*
25
26 421 and *Jobaria*. Given our new findings, it is possible that both broad-crowned and narrow-
27
28 422 crowned sauropods varied in neck length depending on other environmental and ecological
29
30 423 parameters, such as the lushness of the habitat (e.g. a larger feeding envelope might be less
31
32 424 necessary in environments where edible plants are plentiful) or the intensity of predation
33
34 425 pressure. Alternatively, neck-driven changes in CoM may have interacted with feeding ecology
35
36 426 in more complex ways. For example, it has been suggested that sauropods with more caudad
37
38 427 CoM positions, such as diplodocids, were more capable of rearing bipedally to reach higher
39
40 428 vegetation, while the more cranial CoM positions may have rendered other taxa incapable of
41
42 429 such extended upright feeding [34]. Given we find that neck enlargement appears primarily
43
44 430 responsible for the more cranial CoM positions in derived sauropods, it is possible that there
45
46 431 was shift away from feeding using a bipedal rearing strategy as neck elongation opened up
47
48 432 increasingly larger feeding envelopes.
49
50
51
52
53
54
55
56
57 433
58
59
60

1
2 434 The temporal-phylogenetic patterns in relative CoM suggested in our analyses appear,
3
4 435 however, to have stronger implications for locomotion. Specifically, more caudad CoM
5
6 436 positions in basal dinosaurs are consistent with the mechanical demands of efficient and
7
8 437 stable bipedalism [13], most obviously by enabling the vertical alignment of the centre of
9
10 438 pressure and CoM while simultaneously maintaining a net extensor moment about the hind
11
12 439 limb joints at mid-stance [35]. Our dataset supports the inference that Late Triassic bipedal
13
14 440 basal sauropodomorphs might have evolved CoM positions 'intermediate' between the more
15
16 441 caudad positions of basal bipedal dinosaurs and the more cranial loci of quadrupedal basal
17
18 442 sauropods (Fig 6), although the small magnitude of this difference relative to our error bars,
19
20 443 and the mixed signals in our raw predictions for individual taxa (Fig 4), mandate caution in
21
22 444 this interpretation.
23
24
25
26
27
28
29
30

31 445
32
33 446 Increasing body size and the evolution of obligate quadrupedality in sauropodomorphs close
34
35 447 to the sauropod radiation (Fig 6) do not appear to be coincident with discrete or sharp shifts
36
37 448 in the relative proportions of individual body segments (even segment lengths, which are not
38
39 449 subject to the same error margins as mass properties). Rather, changes in segment
40
41 450 proportions reflect the gradual cranial trend in overall CoM that started in basal
42
43 451 sauropodomorphs, with continued increases in the length and masses of the neck and
44
45 452 pectoral limbs, and relative decreases in the pelvic limbs and head (Fig 7). Interestingly,
46
47 453 although relative tail masses decreased slightly, relative tail length continued to increase in
48
49 454 basal sauropods (Fig 7), with extreme elongation in diplodocids [1], which probably accounts
50
51 455 for the absence of a notable cranial shift in overall CoM in association with increased body
52
53 456 size and quadrupedality in this lineage (Figs 4, 6, see also Figs S4 in ESM1).
54
55
56
57
58
59
60

1
2 458 The most striking link to locomotor evolution is the marked craniad shift in CoM in
3
4 459 titanosauriform sauropods during the Late Jurassic (ca. 160Ma). The magnitude of this cranial
5
6 460 shift is such that highly disparate skeletal:body volume ratios would be required to eliminate
7
8 461 it completely (Figs 6, 8), although clearly moderate disparity in skeletal:body volume ratios
9
10 462 could dilute this apparently sudden shift such that it falls more in line as a continuation of the
11
12 463 gradual craniad trend in CoM positions seen throughout the Jurassic (Fig 6). These cranial
13
14 464 CoM positions, underpinned by increased neck size and maintained into the Cretaceous, are
15
16 465 the most extreme positions in Sauropodomorpha (Fig 6), and appear to be temporally
17
18 466 coincident with the widespread appearance of ‘wide-gauge’ sauropod trackways in the fossil
19
20 467 record [36-38]. The Jurassic sauropod footprint record is dominated by ‘narrow-gauge’
21
22 468 trackways in which opposing prints are beneath the body, close to the body mid-line. In
23
24 469 contrast, ‘wide-gauge’ trackways, in which opposing prints are placed well lateral of the mid-
25
26 470 line, dominate the Cretaceous trackway record, seemingly reflecting the emergence and
27
28 471 diversification of Titanosauriformes [36-38].
29
30
31
32
33

34 472
35
36

37 473 Wilson and Carrano [37] proposed that titanosaurs (or a slightly more inclusive grouping of
38
39 474 titanosauriforms [36]) possessed anatomical specializations in their limb girdles and long
40
41 475 bones, as well as an overall wider body that led to the wide-gauge locomotion recorded in
42
43 476 fossil trackways. It is interesting that the predominantly neck-driven craniad shift we have
44
45 477 identified in Titanosauriformes is not concurrent with significant shifts in the relative mass or
46
47 478 gross dimensions of limb segments (Fig 7). Our data indicate that pectoral limb lengths
48
49 479 increased in Early–Middle Jurassic Eusauropoda, and pelvic limb lengths continued to shorten
50
51 480 until slightly later Eusauropoda (*Mamenchisaurus* node, ~174 Ma). However, subsequently,
52
53 481 pelvic and pectoral limbs stabilized at similar relative lengths (~ 0.1 body masses^{1/3}) prior to
54
55 482 the sharp craniad shift in the Late Jurassic. Broadly similar patterns are evident for limb
56
57
58
59
60

1
2 483 masses. Pectoral limb masses increased to a peak of ~ 0.03 body mass in Middle Jurassic
3
4 484 eusauropods (*Jobaria* node, ~ 169 Ma) before declining to ~ 0.02 body mass (similar to
5
6 485 estimated overall pelvic limb mass) in Late Jurassic Titanosauriformes (~ 162 Ma). Our newly
7
8 486 identified neck-driven craniad shift in overall CoM (Figs 6-7) pre-dates the anatomical
9
10 487 specializations noted in titanosaur limb girdles and long bones [37], perhaps suggesting that
11
12 488 these osteological changes, and wide-gauge locomotion in general, were responsive to neck
13
14 489 elongation and craniad CoM migration. The observation that CoM position remained relatively
15
16 490 stable after the evolution of modified limb girdles and long bones in titanosaurs provides
17
18 491 further indirect support for this argument.
19
20
21
22

23 492

24
25 493 Tail reduction in dinosaurs has previously been associated with a reduction in the size of the
26
27 494 caudofemoralis longus (CFL) muscle, which serves as the principal locomotor muscle in most
28
29 495 non-avian Reptilia [13]. It is plausible that tail reduction in sauropods is indicative of the
30
31 496 decreasing importance of the CFL during locomotion in animals with a more craniad CoM.
32
33 497 Indeed, within sauropods, tail reduction is most extreme in derived titanosaurs [1], and based
34
35 498 on qualitative osteological analysis previous workers have hypothesized a reduction in the
36
37 499 size of the CFL during titanosaur evolution [39-40]. Furthermore, these taxa also show a
38
39 500 number of instances of enlarged or even novel muscle attachments on the pectoral girdle and
40
41 501 forelimb in comparison to other sauropods [2, 41-42]. The significant craniad shift in CoM in
42
43 502 Titanosauriformes revealed by our new whole-body analysis provides a link between these
44
45 503 anatomical patterns and suggests a systematic shift in locomotor anatomy (see discussion
46
47 504 below), with derived Titanosauriformes possessing a more craniad CoM and enlarged
48
49 505 forelimb musculature [2, 41-42], but reduced tail-based hindlimb retractors [39-40]. Larger
50
51 506 forelimb musculature would be expected in animals with a more cranially positioned CoM
52
53 507 (reflecting more weight borne on the forelimbs), and would be beneficial in terms of
54
55
56
57
58
59
60

1
2 508 countering reduced effective mechanical advantage of the limbs (medio-laterally) in the more
3
4 509 sprawled postures suggested by wide-gauge trackways.

5
6 510

7
8 511 In contrast to these hypotheses, Henderson [5] proposed that size-correlated changes in body
9
10 512 shape, “independent of clade” (i.e. phylogeny), might have instead been responsible for
11
12 513 differences in trackway gauge within sauropods. Specifically, Henderson [5] suggested that
13
14 514 the body’s CoM shifted forward as body size increased, and subsequently this more cranially
15
16 515 positioned CoM favoured wide-gauge locomotion. Although we find a relatively strong
17
18 516 correlation between whole-body mass and CoM in our phylogenetic patterns (Figs 6-7), our
19
20 517 raw dataset shows a weak positive correlation between body size and CoM position within
21
22 518 sauropodomorphs, with considerable scatter about the best-fit lines (Fig 5). Overall, our
23
24 519 larger and more phylogenetically and temporally widespread dataset exhibits a much
25
26 520 stronger phylogenetic-temporal signal for CoM disparity in sauropodomorphs (Figs 6-7),
27
28 521 rather than purely size-driven trends, which is consistent with the pattern of locomotor
29
30 522 evolution recorded by trackway gauge width [36-38].
31
32
33
34
35

36 523

37
38
39 524 Quantitative palaeoecological analysis indicates that titanosauriform body fossils and wide-
40
41 525 gauge trackways are found primarily in inland palaeoenvironments, whereas non-titanosaurs
42
43 526 and narrow-gauge trackways are often recovered in coastal palaeoenvironments [36]. It is
44
45 527 tempting to speculate that our strong support for a concomitant cranial shift in CoM might
46
47 528 provide the morphological mechanism for an evolutionary change in locomotion (narrow-
48
49 529 gauge to wide-gauge), which is in turn connected to shifts in habitat preferences that
50
51 530 facilitated the radiation of titanosaurs during the Cretaceous, while all other sauropod
52
53 531 lineages dwindled and ultimately went extinct by the early Late Cretaceous (Fig 1). However,
54
55 532 such a scenario remains highly speculative, particularly in the absence of a clear mechanistic
56
57
58
59
60

1
2 533 link between CoM and quadrupedal gait.

3
4
5 534

6
7
8 535 Modifying weight distribution in autonomous quadrupedal robots has been shown to
9
10 536 systematically alter gait patterns, with weighted forelimbs producing lateral sequence gaits
11
12 537 and weighted hindlimbs generating diagonal sequence gaits [43]. This link between mass
13
14 538 distribution and gait has yet to be investigated in living quadrupedal animals, and these
15
16 539 results may not have direct relevance for sauropods given that the CoM shifts (Fig 6) appear
17
18 540 to be driven predominantly by changes in the axial body segments, rather than the limbs (Fig
19
20 541 7), although it is possible that titanosaurs may have evolved more muscular pectoral girdles
21
22 542 [2, 41-42] and reduced hip extensor musculature [39-40]. Clearly more data on how CoM
23
24 543 interacts with locomotor biomechanics in living quadrupedal animals is needed to better
25
26 544 inform studies of extinct taxa. However, the uniqueness of the sauropod body plan in general,
27
28 545 and the predominant role of their characteristically elongate neck in driving the evolutionary
29
30 546 history of their body plan (Figs 6-7), limit the extent to which extant taxa can serve as direct
31
32 547 analogues for sauropod dinosaurs. This means that more direct modeling approaches,
33
34 548 supported by basic principles established in extant animals, are likely to be key to addressing
35
36 549 these and other controversies to further our understanding of the links between functional
37
38 550 anatomy, ecology and macroevolutionary diversity in sauropodomorph dinosaurs.
39
40
41
42
43
44

45 551

46 47 48 552 **CONCLUSIONS**

49
50
51
52 553 Applying any consistent skeleton:body volume ratio to the sample of taxa modeled in this
53
54 554 study yields patterns in body shape evolution that appear concurrent with major
55
56 555 macroevolutionary and biomechanical events in sauropodomorph history (Fig. 6). A caudad
57
58 556 shift in centre-of-mass in Middle Triassic Saurischia, associated with the evolution of
59
60

1
2 557 bipedalism in various dinosaur lineages, was reversed in Late Triassic sauropodomorphs. A
3
4 558 craniad centre-of-mass shift coincided with the evolution of quadrupedalism in the Late
5
6 559 Triassic, followed by a more striking craniad shift in Late Jurassic–Cretaceous
7
8 560 titanosauriforms, which included the largest sauropods (Fig. 6). These craniad CoM shifts are
9
10 561 strongly correlated with neck enlargement (Fig. 7), which has long been considered the most
11
12 562 important innovation in sauropod evolution and pivotal to their gigantism. However all
13
14 563 predictions are associated with a high degree of uncertainty resulting from incomplete
15
16 564 skeletal remains, the absence of soft tissue preservation in fossils, and a relatively low sample
17
18 565 size that results in long phylogenetic branch lengths (Figs 6). Currently, uncertainty in the
19
20 566 relative size of body segment volumes represents the most limiting factor in the robustness of
21
22 567 CoM estimates, and clearly additional data from living archosaurs is required to better
23
24 568 constrain confidence intervals in skeleton:body volume ratios applied to extinct taxa. Overall
25
26 569 this study highlights the difficulty of reconstructing the overall pattern of body shape
27
28 570 evolution in sauropodomorphs, and by inference all fossil vertebrates, with high degree of
29
30 571 confidence.
31
32
33
34
35
36
37
38
39

572

573 **ACKNOWLEDGEMENTS**

574 We thank Matt Lamanna, Lacie Ballinger, Bill Simpson, Pete Makovicky, Emma Schachner,

575 Marcelo Reguero, Alejandro Kramarz, D. Ray Wilhite and Derrick Braithwaite for help

576 digitizing specimens, and Qi Zhao for assisting with measurements of *Mamenchisaurus*.

577 Orlando Grillo supplied the *Staurikosaurus* model to J.R.H., and Heinrich Mallison supplied the

578 *Plateosaurus* model to J.R.H. Tim Rowe, Nicolás Campione and Jeff Wilson are thanked for

579 their critical and thoughtful reviews.

580

1
2 581 **Author Contributions**
3
4

5 582 K.T.B., P.L.F., V.A., S.L.B., A.O., W.I.S., C.S., and K.A.S. digitized fossil material. K.T.B. constructed
6
7 583 and analyzed volumetric reconstructions. V.A. and K.T.B. performed phylogenetic
8
9 584 optimization and statistical analysis. All authors contributed to the manuscript and approved
10
11 585 the final version.
12
13

14
15 586
16
17

18 587 **References**
19
20

- 21 588 1. Wilson JA. Sauropod dinosaur phylogeny: critique and cladistics analysis. *Zool. J. Linn. Soc.*
22
23 589 2002; 136, 217-276.
24
25
26 590 2. Upchurch P, Barrett PM, Dodson P. Sauropoda. In: Weishampel DB, Dodson P, Osmólska H,
27
28 591 editors. The Dinosauria (2nd Ed.). Berkeley: University of California Press; 2004, pp. 259–
29
30 592 324.
31
32
33 593 3. Sander PM, Christian A, Clauss M, Fechner R, Gee CT, Griebeler EM, *et al.* Biology of the
34
35 594 sauropod dinosaurs: the evolution of gigantism. *Biol. Rev.* 2010; 86, 117-160.
36
37 595 4. Benson RBJ, Campione NE, Carrano MT, Mannion PD, Sullivan C, Upchurch P, Evans, DC.
38
39 596 Rates of dinosaur body mass evolution indicate 170 million years of sustained ecological
40
41 597 innovation on the avian stem lineage. *PLoS Biology* 2014; **12** e1001853. DOI:
42
43 598 10.1371/journal.pbio.1001853.
44
45
46 599 5. Henderson DM. Burly gaits: centres of mass, stability, and the trackways of sauropod
47
48 600 dinosaurs. *J. Verte. Pal.* 2006; 4, 907-921.
49
50
51 601 6. Henderson DM. Tippy punters: sauropod dinosaur pneumaticity, buoyancy and aquatic
52
53 602 habits. *Proc. Roy. Soc. B* 2004; 271, S180-183.
54
55
56 603 7. Rauhut, O, Fechner, R, Remes, K, Reis, K. How to get big in the Mesozoic: the evolution of
57
58 604 the sauropodomorph body plan. In Klein N, Remes K, Gee CT, Sander PM, editors. *Biology*
59
60

- 1
2 605 of the sauropod dinosaurs: Understanding the life of giants. Bloomington: Indiana
3
4 606 University Press; 2011. pp. 119–149.
5
6 607 8. Bell MA, Lloyd GT. Strap: an R package for plotting phylogenies against stratigraphy and
7
8 608 assessing their stratigraphic congruence. *Palaeontology*. 2014; 58, 379–389.
9
10 609 9. Sellers WI, Hepworth-Bell J, Falkingham PL, Bates KT, Brassey CA, Egerton V, Manning PL.
11
12 610 Minimum convex hull mass estimations of complete mounted skeletons. *Biology Letters*
13
14 611 2012; doi: 10.1098/rsbl.2012.0263.
15
16 612 10. Bates KT, Falkingham PL, Macaulay S, Brassey CA, Maidment SCR. Downsizing a gaint: re-
17
18 613 evaluating *Dreadnoughtus* body mass. *Biology Letters* 2015; DOI: 10.1098/rsbl.2015.0215.
19
20 614 11. Bates KT, Manning PL, Hodgetts D, Sellers WI. Estimating the body mass of dinosaurs
21
22 615 using laser imaging and 3D computer modelling. *PLoS ONE* 2009; 4(2), e4532. doi:
23
24 616 10.1371.
25
26 617 12. Bates KT, Falkingham PL, Breithaupt BH, Hodgetts D, Sellers WI, Manning PL. How big
27
28 618 was ‘Big Al’? Quantifying the effect of soft tissue and osteological unknowns on mass
29
30 619 predictions for *Allosaurus* (Dinosauria: Theropoda). *Palaeontological Electronica* 2009;
31
32 620 12(3): 14A, p. 33 (2009).
33
34 621 13. Allen V, Bates KT, Zhiheng L, Hutchinson JR. Linking the evolution of body shape and
35
36 622 locomotor biomechanics in bird-line archosaurs. *Nature* 2013; 497, 104-107.
37
38 623 14. Allen V, Paxton H, Hutchinson JR. 2009. Variation in centre of mass estimates for extant
39
40 624 sauropsids and its importance for reconstructing inertial properties in extinct archosaurs.
41
42 625 *Anatomical Record* 292, 1442-1461.
43
44 626 15. Yates AM, Kitching JW. The earliest known sauropod dinosaur and the first steps towards
45
46 627 sauropod locomotion. *Proc. Roy. Soc. B* 2003; 270, 1753-1758.
47
48 628 16. Falkingham PL. Acquisition of high resolution three-dimensional models using free, open-
49
50 629 source, photogrammetric software. *Palaeontologia Electronica* 2012; 15, 1; 1T:15p.
51
52
53
54
55
56
57
58
59
60

- 1
2 630 17. Stevens KA. Articulation of sauropod necks: Methodology and mythology. *PLoS ONE* 2013;
3
4 631 8(10): e78572. doi:10.1371/journal.pone.0078572.
5
6 632 18. Stevens KA, Parrish JM. Neck posture and feeding habits of two Jurassic sauropods.
7
8 633 *Science* 1999; 284, 798-800.
9
10 634 19. Taylor MP, Hone DWE, Wedel MJ, Naish D. The long necks of sauropods did not evolve
11
12 635 primarily through sexual selection. *J. Zool.* 2011; doi:10.1111/j.1469-7998.2011.00824.x.
13
14 636 20. Taylor MP, Wedel MJ. The effect of intervertebral cartilage on neutral posture and range
15
16 637 of motion in the necks of sauropod dinosaurs. *PLoS ONE* 2013; 8(10), e78214.
17
18 638 doi:10.1371/journal.pone.0078214.
19
20 639 21. Christian A, Dzemski G. 2011 Neck posture in sauropods. In *Biology of the sauropod*
21
22 640 *dinosaurs: understanding the life of giants* (eds Klein N, Remes K, Gee CT, Sander PM), pp.
23
24 641 251–260. Bloomington, IN: Indiana University Press.
25
26 642 22. Wedel MJ. Postcranial Skeletal Pneumaticity in Sauropods and Its Implications for Mass
27
28 643 Estimates. In: Wilson JA, Curry-Rogers KA, editors. *The sauropods: evolution and*
29
30 644 *paleobiology*. Berkeley: University of California Press; 2005. pp. 201–228.
31
32 645 23. Paradis, E., Claude, J., Strimmer, K. 2004 APE: analyses of phylogenetics and evolution in R
33
34 646 language. *Bioinformatics*. 20, 289-290.
35
36 647 24. Revell, L. J. 2012 phytools: an R package for phylogenetic comparative biology (and other
37
38 648 things). *Methods in Ecology and Evolution*. 3, 217-223.
39
40 649 25. Felsenstein J. Phylogenies and the comparative method. *The American Naturalist* 1985;
41
42 650 125, 1-15.
43
44 651 26. Sereno PC, Wilson JA, Witmer LM, Whitlock JA, Maga A et al. Structural extremes in a
45
46 652 Cretaceous dinosaur. *PLoS ONE* 2007; 2: e1230.
47
48 653 27. Curry Rogers KA. Titanosauria: a phylogenetic overview. In: Curry Rogers KA, Wilson JA,
49
50 654 editors. *The sauropods: evolution and paleobiology*. Berkeley; University of California
51
52 655 Press; 2005. pp 50–103.
53
54
55
56
57
58
59
60

- 1
2 656 28. Preuschoft H, Hohn B, Stoinski S, Witzel U. 2011. Why so huge? Biomechanical reasons for
3
4 657 the acquisition of large size in sauropod and theropod dinosaurs. In *Biology of the*
5
6 658 *sauropod dinosaurs: understanding the life of giants* (eds Klein N, Remes K, Gee CT, Sander
7
8 659 PM), pp. 197-218. Bloomington, IN: Indiana University Press.
- 9
10 660 29. Button DJ, Rayfield EJ, Barrett PM. Cranial biomechanics underpins high sauropod
11
12 661 diversity in resource-poor environments *Proc. Roy. Soc. B* 2014; doi:
13
14 662 10.1098/rspb.2014.2114.
- 15
16
17 663 30. Young MT, Rayfield EJ, Holliday CM, Witmer LM, Button DJ, Upchurch P, Barrett PM.
18
19 664 Cranial biomechanics of *Diplodocus* (Dinosauria, Sauropoda): testing hypotheses of
20
21 665 feeding behaviour in an extinct megaherbivore. *Naturwissenschaften* 2012; 99, 637–643.
- 22
23
24 666 31. Calvo JO. 1994 Jaw mechanics in sauropod dinosaurs. *Gaia* 10, 183 – 193.
- 25
26
27 667 32. Christiansen P. 2000 Feeding mechanisms of the sauropod dinosaurs *Brachiosaurus*,
28
29 668 *Camarasaurus*, *Diplodocus* and *Dicraeosaurus*. *Hist. Biol.* 14, 137 – 152.
30
31 669 (doi:10.1080/10292380009380563)
- 32
33 670 33. Upchurch P, Barrett PM. 2000 The evolution of sauropod feeding mechanisms. In
34
35 671 *Evolution of herbivory in terrestrial vertebrates: perspectives from the fossil record* (ed.
36
37 672 H-D Sues), pp. 79 – 122. Cambridge, UK: Cambridge University Press.
- 38
39
40 673 34. Mallison H. 2011. Rearing giants: Kinetic-dynamic modelling of sauropod bipedal and
41
42 674 tripodal poses. In *Biology of the sauropod dinosaurs: understanding the life of giants* (eds
43
44 675 Klein N, Remes K, Gee CT, Sander PM), pp. 237–250. Bloomington, IN: Indiana University
45
46 676 Press.
- 47
48
49 677 35. Hutchinson JR. Biomechanical modelling and sensitivity analysis of bipedal running. I.
50
51 678 Extant taxa. *J. Morph.* 2004; 262, 421-440.
- 52
53
54 679 36. Mannion PD, Upchurch P. A quantitative analysis of environmental associations in
55
56 680 sauropod dinosaurs. *Paleobiology* 2010; 36: 253-282.
- 57
58
59
60

- 1
2 681 37. Wilson JA, Carrano MT. Titanosaurs and the origin of “wide-gauge” trackways: a
3
4 682 biomechanical systematic perspective on sauropod locomotion. *Paleobiology* 1999; 25,
5
6 683 252-267.
7
8
9 684 38. Wilson JA. Integrating ichnofossil and body fossil records to estimate locomotor posture
10
11 685 and spatiotemporal distribution of early sauropod dinosaurs: a stratocladistic approach.
12
13 686 *Paleobiology* 2005; 31, 400-423.
14
15
16 687 39. Salgado L, García R, Variación morfológica en la secuencia de vértebras caudales de
17
18 688 algunos saurópodos titanosaurios. *Revista Española de Paleontología* 2002; 17, 211-216.
19
20 689 40. Ibiricu LM, Lamanna MC, Lacovara KJ. The influence of caudofemoral musculature on the
21
22 690 titanosaurian (Saurischia: Sauropoda) tail skeleton: morphological and phylogenetic
23
24 691 implications. *Historical Biology* 2014; 26, 454-471.
25
26
27 692 41. Borsuk-Bialynicka M. A new camarasaurid sauropod *Opisthocoelicaudia skarzynskii* gen.
28
29 693 n., sp. n. from the Upper Cretaceous of Mongolia. *Palaeontologica Polonica* 1977; 37, 5-63.
30
31 694 42. Otero A. The appendicular skeleton of *Neuquensaurus*, a Late Cretaceous saltosaurine
32
33 695 sauropod from Patagonia, Argentina. *Acta Palaeontologica Polonica* 2010; 55, 399-426.
34
35
36 696 43. Owaki D, Kano T, Nagasawa K, Tero A, Ishiguro A. Simple robot suggests physical
37
38 697 interlimb communication is essential for quadruped walking. *J. Roy. Soc. Interface* 2013;
39
40 698 0120669.
41
42
43 699
44
45
46
47
48
49
50
51
52
53
54
55
56
57
58
59
60

1
2 700 **Figure Captions**
3
4

5 701 **Figure 1.** Time-calibrated phylogeny showing taxa included in this study (partly generated
6
7 702 using [8]), with silhouettes of the convex hull volumetric models in left lateral view.

8
9 703 Silhouettes not to scale.
10
11

12 704

13
14 705 **Figure 2.** Reconstructed sauropod dinosaur (*Dicraeosaurus*) body volumes. We used an
15
16 706 automated algorithm to produce an initial minimum convex hull volume (bottom model,
17
18 707 green) around digitized fossil skeletons to minimize subjectivity [9-10]. Two geometrically
19
20 708 similar expansions of this minimal volume were produced ('Plus21%' middle, gray [in
21
22 709 accordance with 9]; 'Maximal' top, red) from which we selected combinations of body
23
24 710 segments that produced the most caudal (left) and cranial (right) CoM positions.
25
26 711

27
28 712

29
30 713 **Figure 3.** Examples of neck orientations used in the sensitivity analyses. *Giraffatitan* model in
31
32 714 right lateral view with neck inclined to (a) 45 degrees and (b) in the osteologically-straight,
33
34 715 undeflected state. In (b) the neck rises at a slope of between 18-27 degrees above the
35
36 716 horizontal (depending upon the reconstruction of the pectoral girdles upon the ribcage)
37
38 717 (Figure 4 in [17]). The pose in (a), on the other hand, corresponds to the familiar giraffe-like
39
40 718 interpretation of macronarian neck posture, wherein the neck rises steeply either by
41
42 719 reconstructing the vertebrae as if wedge-shaped at the base (as in the Berlin reconstruction)
43
44 720 or by suggesting they habitually bent their necks to the limit of dorsiflexion at the base [19-
45
46 721 20]).
47
48 722

49
50 723

51
52 724 **Figure 4.** Raw CoM predictions for all taxa with normalization conducted using (a) distance
53
54 725 cranial to the hip divided by body mass^{0.33} and (b) as a fraction of gleno-acetabular distance.
55
56 726

57 727 Data plotted comes from the Plus21% model iteration with densities in the neck and thoracic
58
59 728
60

1
2 725 segments of sauropodomorph models varied to represent the effects of differential levels of
3
4 726 pneumatic air space (50%, 70% and 90%) within the vertebral column in these regions.
5
6
7
8
9

727

10
11 728 **Figure 5.** Reduced major axis regression of CoM against mean body mass using raw data for
12
13 729 all taxa modeled in this study with CoM normalized by **(a)** distance in front of the hip divided
14
15 730 by body mass^{0.33} and **(b)** as a fraction of gleno-acetabular distance. Regression statistics for
16
17 731 **(a)** distance in front of the hip divided by body mass^{0.33} are: all taxa RMA regression slope =
18
19 732 2.52e-06, intercept = 0.034, r² = 0.157, p = 0.068; Sauropodomorpha RMA regression slope =
20
21 733 2.65e-06, intercept = 0.276, r² = 0.172, p = 0.098; Sauropoda RMA regression slope = 2.68e-
22
23 734 06, intercept = 0.027, r² = 0.088, p = 0.282. Regression statistics for **(b)** as a fraction of gleno-
24
25 735 acetabular distance are: all taxa RMA regression slope = 1.83e-05, intercept = 0.258, r² =
26
27 736 0.327, p = 0.005; Sauropodomorpha RMA regression slope = 1.85e-05, intercept = 0.244, r² =
28
29 737 0.243, p = 0.045; Sauropoda RMA regression slope = 1.80e-05, intercept = 0.253, r² = 0.138, p
30
31 738 = 0.172.
32
33
34
35
36

739

37
38
39
40 740 **Figure 6.** Estimated evolutionary patterns in whole-body CoM position along the
41
42 741 craniocaudal axis of the body with data normalized by **(a)** distance in front of the hip divided
43
44 742 by body mass^{0.33} and **(b)** as a fraction of gleno-acetabular distance.
45
46
47

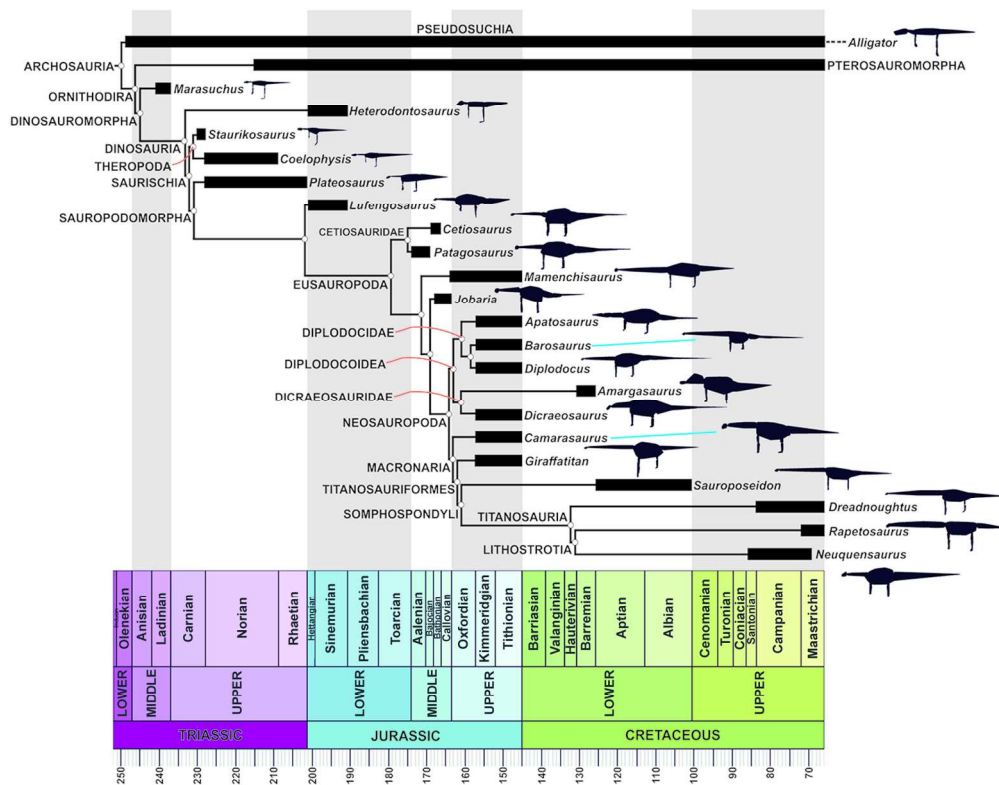
743

48
49
50
51 744 **Figure 7.** Estimated evolutionary patterns in individual body segment properties, expressed
52
53 745 as (a) segment length normalized by body mass^{0.33}, (b) segment mass as a proportion of body
54
55 746 mass, (c) distance of segment CoM position from the hip normalized by body mass^{0.33}, and (d)
56
57 747 segment first mass moment normalized by body mass^{1.33}.
58
59
60

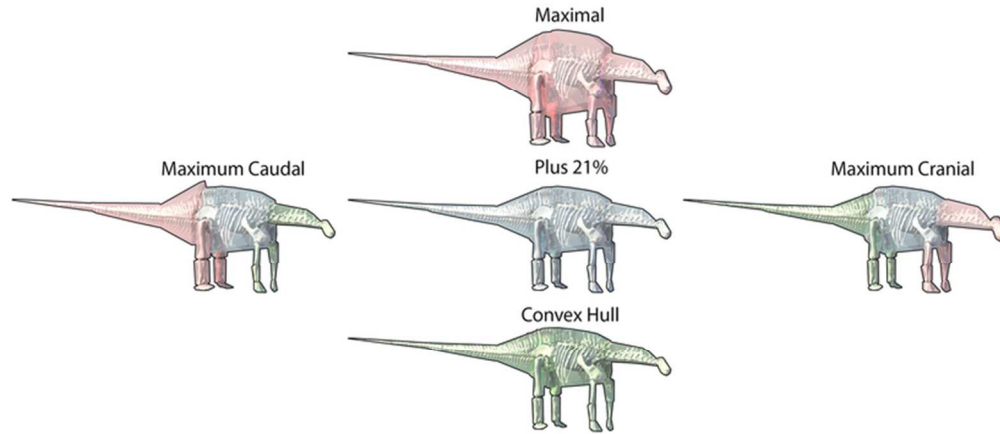
1
2 748

3
4 749 **Figure 8.** Comparison of our original estimated evolutionary patterns in whole-body CoM
5
6 750 position (Fig 6) to alternative reconstructions with inclined necks in macronarian taxa and
7
8 751 increased/decreased neck lengths in *Sauroposeidon*, *Dreadnoughtus* and *Neuquensaurus*.
9

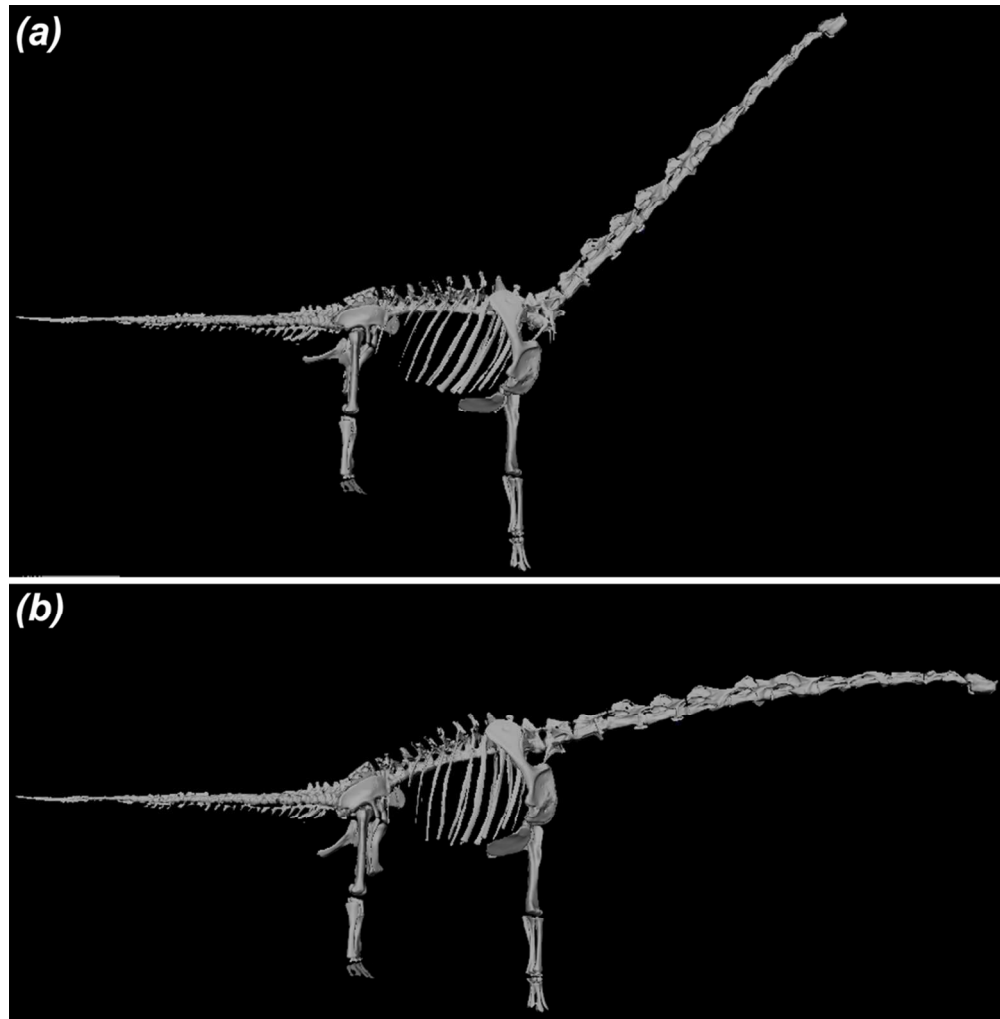
10
11
12
13
14
15
16
17
18
19
20
21
22
23
24
25
26
27
28
29
30
31
32
33
34
35
36
37
38
39
40
41
42
43
44
45
46
47
48
49
50
51
52
53
54
55
56
57
58
59
60



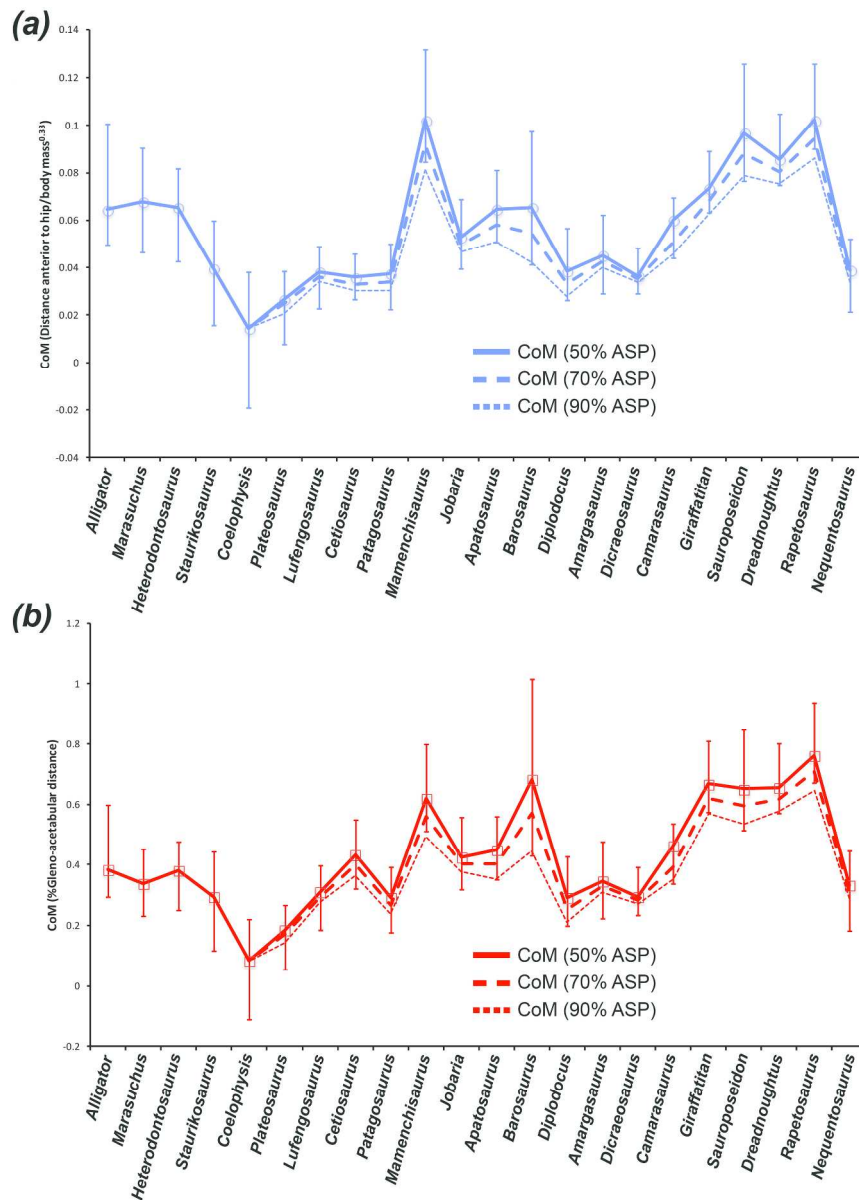
Time-calibrated phylogeny showing taxa included in this study (partly generated using [8]), with silhouettes of the convex hull volumetric models in left lateral view. Silhouettes not to scale.
160x125mm (300 x 300 DPI)



Reconstructed sauropod dinosaur (*Dicraeosaurus*) body volumes. We used an automated algorithm to produce an initial minimum convex hull volume (bottom model, green) around digitized fossil skeletons to minimize subjectivity [9-10]. Two geometrically similar expansions of this minimal volume were produced ('Plus21%' middle, gray [in accordance with 9]; 'Maximal' top, red) from which we selected combinations of body segments that produced the most caudal (left) and cranial (right) CoM positions.
69x29mm (300 x 300 DPI)

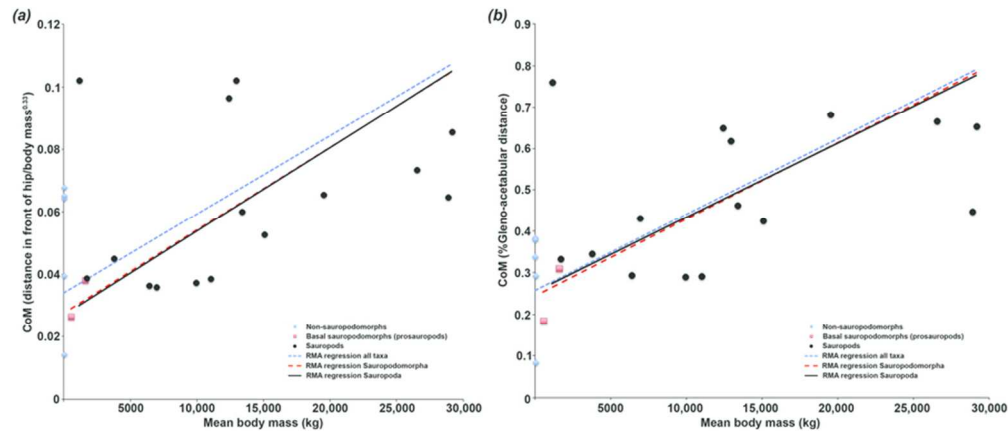


Examples of neck orientations used in the sensitivity analyses. Giraffatitan model in right lateral view with neck inclined to (a) 45 degrees and (b) in the osteologically-straight, undeflected state. In (b) the neck rises at a slope of between 18-27 degrees above the horizontal (depending upon the reconstruction of the pectoral girdles upon the ribcage) (Figure 4 in [17]). The pose in (a), on the other hand, corresponds to the familiar giraffe-like interpretation of macronarian neck posture, wherein the neck rises steeply either by reconstructing the vertebrae as if wedge-shaped at the base (as in the Berlin reconstruction) or by suggesting they habitually bent their necks to the limit of dorsiflexion at the base [19-20].
91x92mm (300 x 300 DPI)



Raw CoM predictions for all taxa with normalization conducted using (a) distance cranial to the hip divided by body mass^{0.33} and (b) as a fraction of gleno-acetabular distance. Data plotted comes from the Plus21% model iteration with densities in the neck and thoracic segments of sauropodomorph models varied to represent the effects of differential levels of pneumatic air space (50%, 70% and 90%) within the vertebral column in these regions.

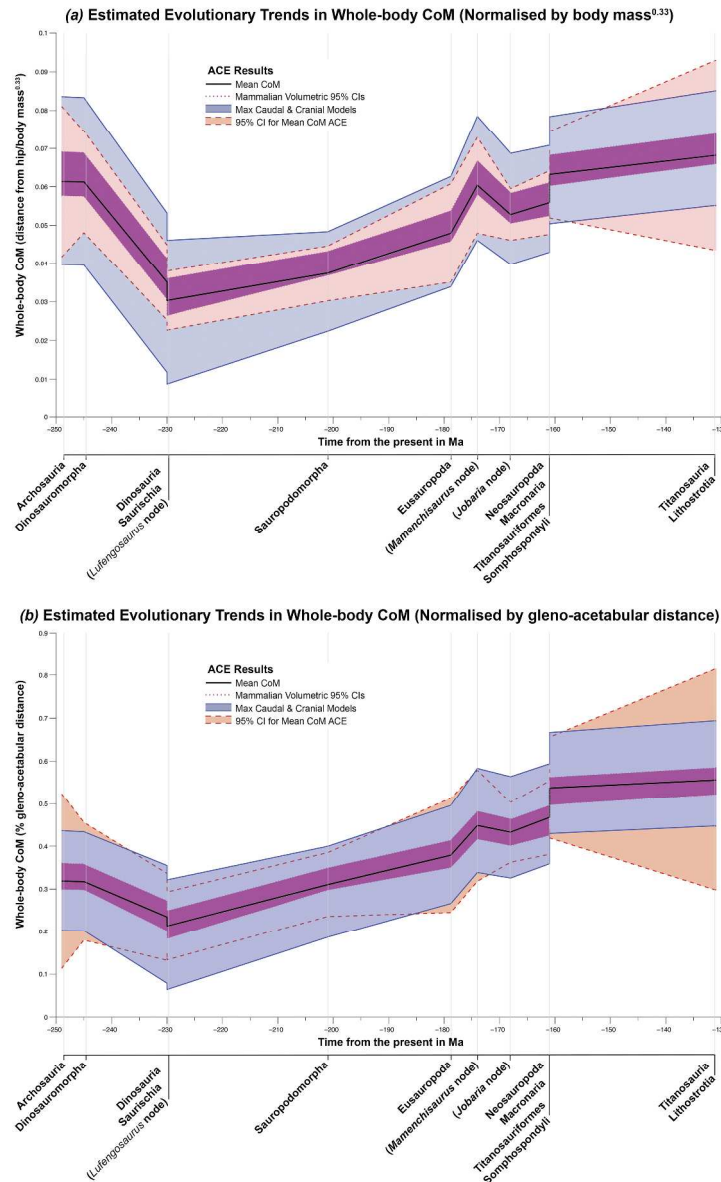
221x307mm (300 x 300 DPI)



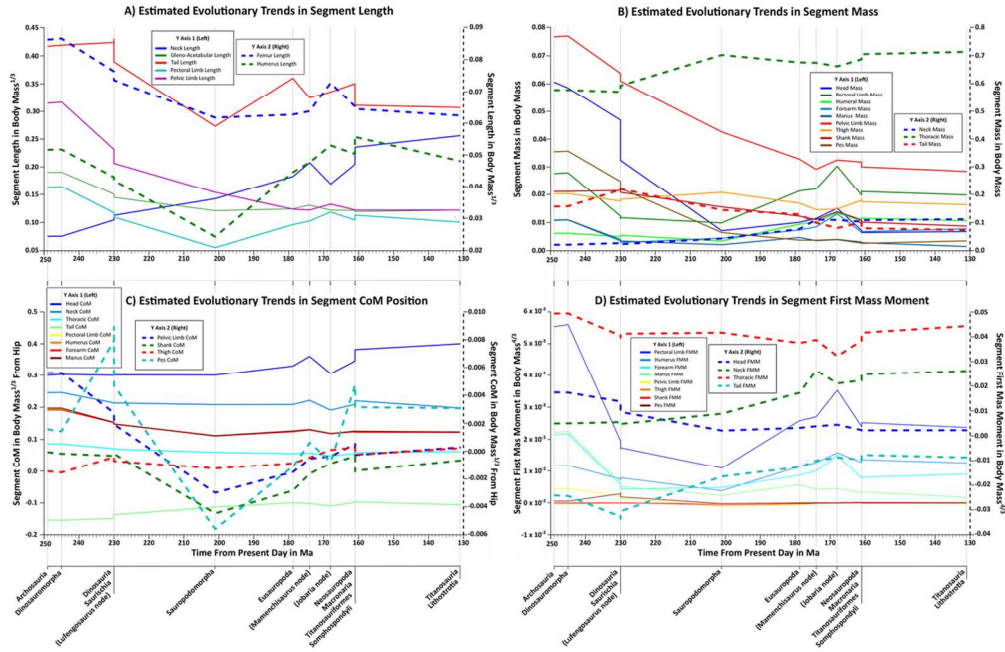
Reduced major axis regression of CoM against mean body mass using raw data for all taxa modeled in this study with CoM normalized by (a) distance in front of the hip divided by body mass^{0.33} and (b) as a fraction of gleno-acetabular distance. Regression statistics for (a) distance in front of the hip divided by body mass^{0.33} are: all taxa RMA regression slope = 2.52×10^{-6} , intercept = 0.034, $r^2 = 0.157$, $p = 0.068$; Sauropodomorpha RMA regression slope = 2.65×10^{-6} , intercept = 0.276, $r^2 = 0.172$, $p = 0.098$; Sauropoda RMA regression slope = 2.68×10^{-6} , intercept = 0.027, $r^2 = 0.088$, $p = 0.282$. Regression statistics for (b) as a fraction of gleno-acetabular distance are: all taxa RMA regression slope = 1.83×10^{-5} , intercept = 0.258, $r^2 = 0.327$, $p = 0.005$; Sauropodomorpha RMA regression slope = 1.85×10^{-5} , intercept = 0.244, $r^2 = 0.243$, $p = 0.045$; Sauropoda RMA regression slope = 1.80×10^{-5} , intercept = 0.253, $r^2 = 0.138$, $p = 0.172$.

76x32mm (300 x 300 DPI)

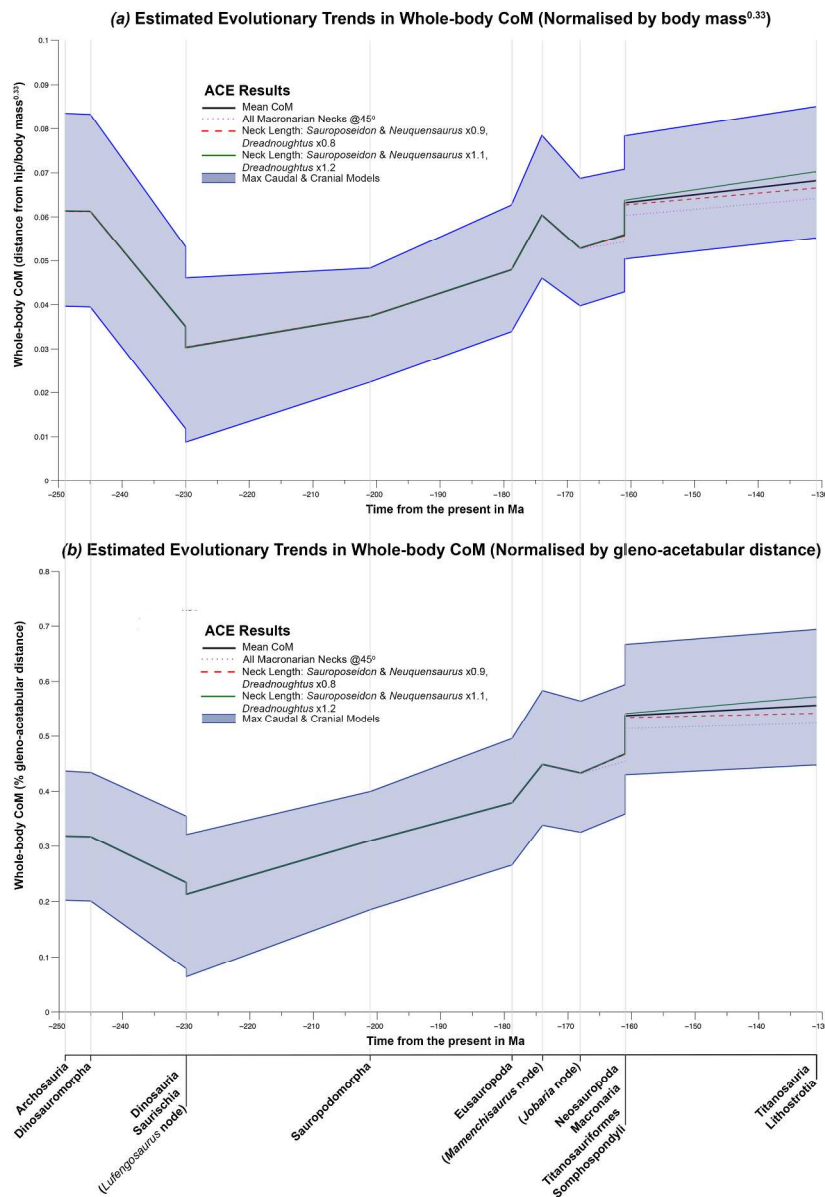
1
2
3
4
5
6
7
8
9
10
11
12
13
14
15
16
17
18
19
20
21
22
23
24
25
26
27
28
29
30
31
32
33
34
35
36
37
38
39
40
41
42
43
44
45
46
47
48
49
50
51
52
53
54
55
56
57
58
59
60



Estimated evolutionary patterns in whole-body CoM position along the craniocaudal axis of the body with data normalised by (a) distance in front of the hip divided by body mass^{0.33} and (b) as a fraction of gleno-acetabular distance.
264x438mm (300 x 300 DPI)



Estimated evolutionary patterns in individual body segment properties, expressed as (a) segment length normalized by body mass^{0.33}, (b) segment mass as a proportion of body mass, (c) distance of segment CoM position from the hip normalized by body mass^{0.33}, and (d) segment first mass moment normalized by body mass^{1.33}.
116x75mm (300 x 300 DPI)



Comparison of our original estimated evolutionary patterns in whole-body CoM position (Fig 6) to alternative reconstructions with inclined necks in macronarian taxa and increased/decreased neck lengths in *Sauroposeidon*, *Dreadnoughtus* and *Neuquensaurus*.
230x332mm (300 x 300 DPI)